Int. J. Heat Mass Transfer Vol. 25, No. 6, pp. 847–861, 1982
Printed in Great Britain

0017-9310/82/060847-15 $03.00/0

EXPERIMENTAL AND ANALYTICAL STUDY OF HEAT TRANSFER AND MIXING IN THERMALLY STRATIFIED BUOYANT FLOWS

R. VISKANTA and M. BEHNIA
Heat Transfer Laboratory, School of Mechanical Engineering
Purdue University, West Lafayette, IN 47907, U.S.A.

(*Received* 16 *December* 1981)

Abstract—Unsteady natural convection in a nonuniformly stratified, finite depth, layer of water heated from below has been studied. Laboratory experiments were performed using a Mach–Zehnder interferometer as a diagnostic tool for measuring temperature and a shadowgraph technique for flow visualization. A 1-dim. model in conjunction with a two-differential equation k–ε turbulence model is used to predict the dynamics of the mixed layer which develops when the thermally stratified fluid is heated from below. Good agreement between data and predictions have been obtained using the model. However, the entrainment processes at the interface between the mixed layer and the stable region as well as turbulence in the interfacial layer must be better understood for more realistic modeling of turbulent natural convection in nonuniformly stratified fluids.

Unsteady natural convection heat transfer and mixing which occur when either a thermally stratified layer of liquid is cooled by air flow over the free surface or a layer of liquid is simultaneously heated by an external radiation source and cooled by air flow over the free surface has been studied both experimentally and analytically. Temperature measurements were made using a Mach–Zehnder interferometer, thermocouples and a thermistor. The flow structure in the fluid was visualized using a black–blue dye and "fish-scales" as tracers, and also by shadowgraphic techniques. An unsteady 1-dim. model has been developed for predicting the temperature structure in water irradiated by an external source and simultaneously cooled by air flow over the surface. Turbulent mixing was calculated using the k–ε model of turbulence. The results obtained show that deposition of radiation in water plays an important role on buoyancy and wind shear induced mixing processes in the surface layers during simultaneous heating by radiation and cooling by convection. The mixed layer depth was overpredicted by the turbulence model because it does not adequately simulate the entrainment process in the interfacial layer between the mixed and stable regions.

NOMENCLATURE

- c, specific heat of fluid;
- D, layer depth;
- F, local radiation flux;
- g, gravitational constant;
- k, thermal conductivity of fluid or kinetic energy of turbulence;
- k_{eff}, effective (molecular plus turbulent) thermal conductivity, $k_{eff} = k + k_t$;
- Pr, Prandtl number;
- p, pressure;
- q, heat flux;
- T, time averaged temperature;
- t, time;
- u, time averaged velocity in the x-direction;
- v, time averaged velocity in the y-direction;
- V_a, air velocity at the center of the channel;
- x, y, coordinates in the horizontal plane;
- z, coordinate in the vertical direction (measured from the bottom for heating from below or measured from the interface when the cooling is from above);

Greek symbols

- α, absorptivity;
- β, thermal expansion coefficient;
- ε, turbulent kinetic energy dissipation;
- λ, wavelength or spectral;
- μ, dynamic viscosity of fluid;
- μ_{eff}, effective (molecular plus turbulent) viscosity of fluid, $\mu_{eff} = \mu + \mu_t$;
- ρ, density of fluid;
- τ, shear stress;
- ϕ, relative humidity of air.

Subscripts

- b, refers to bottom of test cell;
- f, refers to heating fluid;
- inc, refers to incident;
- 0, refers to initial;
- s, refers to surface;
- t, refers to turbulent.

1. INTRODUCTION

AN UNDERSTANDING of the flow and thermal structures in fluids heated and/or cooled from above is needed in many areas of current engineering and geophysical interest. Examples include natural waterbodies (e.g. lakes, ponds, reservoirs and estuaries), shallow and salt gradient stratified ponds, artificial lakes for seasonal energy storage, sensible energy storage systems [1–7]

and many others. For example, in natural waterbodies the flow and thermal structures have important effects on chemical and physical properties, dissolved oxygen, biological and chemical oxygen demand, aquatic life, chemical and thermal pollution, ecology and mixing processes in water. Energy transfer and mixing processes in water often provide the basic information that leads to a better understanding of such phenomena. The thermal conditions in shallow and salt gradient stratified solar ponds [2, 5, 6] are strongly affected by the existence of buoyancy-induced flows. Such flows exist when the liquid layer is destabilized due to heating from below and/or cooling from above. In ponds the heating from below is produced by the absorption of solar radiation by the pond bottom. The maintenance of stratification in solar ponds is a problem of current concern. The behavior of the hot-cold transition zone ('thermocline') and the maintenance of stratification between the hot and cold fluid layers in large thermal energy storage units [7] and in artificial reservoirs [3] for residential and industrial process heat storage are topics of current research activity. The work reported in this paper is concerned with experimental and analytical modeling of heat transfer in buoyant flows of the type that arises in impounded waters such as lakes, ponds and reservoirs, as well as solar ponds.

Energy transfer processes of internal absorption of solar radiation, buoyancy and shear induced mixing, and advection strongly influence the hydrodynamic and thermal conditions in waters. They are difficult to model because the processes are very complicated. There are both experimental and theoretical difficulties in scaling natural transport processes, and the interactions at the air-water interface cannot be adequately simulated in a laboratory.

Laboratory modeling of atmospheric penetrative convection in a tank of water which was continuously and uniformly stratified (e.g. linearly varying temperature with depth) was performed by Deardorff *et al.* [8] and Heidt [9]. The water was heated from below by circulating a warm fluid through passages at the bottom of the tank. In a careful laboratory study Deardorff *et al.* [8] have measured the vertical profiles of horizontally averaged temperatures and heat fluxes and have determined the mixed layer growth. A similar study was performed by Heidt [9] who in addition employed a shadowgraphic technique to observe the region between the unstable and stratified water layers. Relatively simple mathematical models have been developed to predict the mixed layer growth in penetrative convection that yielded good agreement with the observations [8, 9]. A detailed experimental study of the steady temperature structure in the top surface thermal boundary layer of quiescent water was reported by Katsaros *et al.* [10]. They have also presented a thorough review of the relevant literature. Buoyancy-driven flows have been discussed by Turner [11] and there is no need to repeat this comprehensive review.

During the past decade there has been great interest in modeling the hydrodynamics and thermodynamics of natural waterbodies as evidenced, for example, by the international seminar [4]. There have been numerous studies concerned with modeling of radiation transport and associated thermal stratification [12, 13], cooling (free) of thermally stratified (by radiation) water from the surface [14, 15], buoyancy-generated flow due to cooling of water from the free surface [10, 15], dynamics of the surface mixed layer [16, 17], and sensible and latent energy transport [18, 19] and also with the effects of waves of a wavy air-water interface on evaporation from the surface [20, 21]. Recent reviews of the internal transport processes in waters and interactions at the air-water interface on both micro and macro turbulence levels [22] as well as of laboratory studies [23] are available and will not be repeated. Experiments concerned with internal transport processes in water and the interactions at the air-water surface have not been reported in the literature.

The purpose of the present paper is to report on an experimental and mathematical modeling of thermal structure and mixing in thermally stratified, buoyant water flows. The emphasis of the work is on laboratory modeling of the buoyancy-driven mixed ('convective') layer dynamics and entrainment of heat and fluid into the mixed layer from the stably stratified region under two conditions: (1) heating from below of a stratified fluid layer and (2) cooling from above of a stratified fluid layer. Thermal stratification of the water layer prior to the experiment was achieved by radiant heating from above and/or cooling from below. The cooling of the water surface from above by convection and latent energy transport was accomplished by forcing air over the free surface. A number of different experiments and supporting analyses have been performed to obtain understanding of the transport processes. Knowledge of the processes intractions between the processes is needed for developing predictive models for such energy related systems as natural and artificial cooling lakes, solar ponds, and long-term energy storage systems.

2. HEATING OF A THERMALLY STRATIFIED FLUID FROM BELOW

2.1. *Experiments*

2.1.1. *Test apparatus.* A Mach-Zehnder interferometer was selected as a diagnostic tool for measuring the unsteady temperature distribution and inferring the fluid motion. The interferometer is an ideal instrument to study 2-dim. transport phenomena [24]. Since the instrument senses differences in the refractive index of a fluid, it requires no physical contact of a foreign object with the fluid and therefore does not disturb or distort the temperature field. The interferometer used in the study was of typical rectangular design with 25 cm dia optics. A He-Ne laser served as a light source, and a system of lenses with 25 cm dia parabolic mirrors produced a collimated beam.

The fluid motion was observed using a shadowgraph technique. This was achieved simply by blocking the collimated beam in the reference leg of the interferometer. The beam in the test leg of the interferometer (which passed through the test cell) created a shadowgraphic image which was photographed. A calibrated thermistor (YS144201 with a 0.2 cm dia bead) was installed approx. 0.6 cm above the inside bottom of the test cell to detect local temperature fluctuations caused by fluid parcels departing from the vicinity of the plate.

A rectangular test cell (Fig. 1) with inside dimensions of 10 cm along the optical path, 25 cm wide, and 20 cm high, was placed in the test leg of the interferometer. Optical quality glass windows, 15 cm wide and 1.5 cm thick, were installed into the Plexiglas walls. A larger test cell would have been desirable but, unfortunately, the choice of diagnostics and the size of the interferometer optics did not permit the use of one. The bottom of the cell was coated with a black paint to simulate a highly absorbing, well defined boundary condition. Two calibrated type-T thermocouples were epoxied into the inlet and outlet tubes of the heat source–sink and a type-T thermocouple was installed in the center of the bottom plate. Styrofoam insulation, 3 cm thick, was used to cover the side walls and the optical windows. The bottom of the heat source–sink was insulated with 2.5 cm thick glass wool. The insulation from the windows could be easily removed in order to take photographs of the interference fringe pattern.

2.1.2. *Procedure and data reduction.* The test cell was cleaned and filled with distilled water, covered, and left undisturbed for some time to eliminate convective currents which are normally present and also to attain a uniform temperature equal to the ambient room temperature. The water was then simultaneously cooled from below and heated from above in order to achieve desired stratification conditions. The water was heated from above by means of two high temperature tungsten filament lamps in parabolic reflectors with known spectral radiation characteristics. The reflectors were designed to provide a radiation beam within a 5 cm wide, 25 cm long rectangular region. The fluid circulated through the passages was supplied from a constant temperature bath and its temperature and flow rate were regulated.

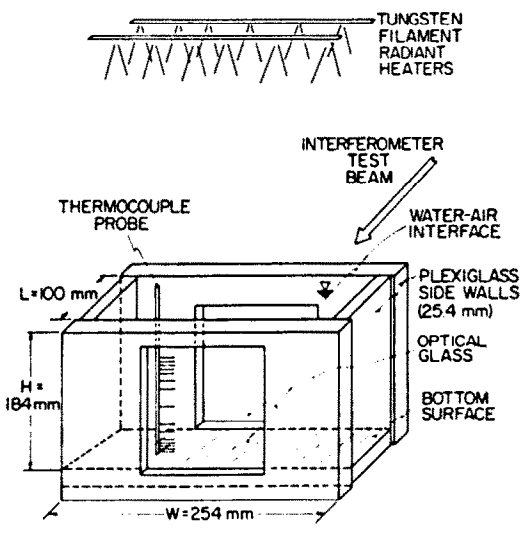

FIG. 1. Schematic diagram of test cell.

After the desired stratification was achieved, the water was then heated from below by circulating a coolant through the heat source–sink from a constant temperature bath. The heating rate was controlled by regulating the coolant flow and inlet temperature to the heat source–sink. The heating rate at the bottom of the test cell was determined from the measured mass flow rate and the temperature drop of the coolant. The rate was corrected for the loss from the source–sink to the ambient laboratory environment through the insulation on the bottom of the cell.

At desired intervals, the interference fringe patterns were photographed with a 35 mm camera, and the reference (as well as other) thermocouple e.m.f. output and the coolant flow rate were simultaneously recorded.

The position of the interference fringes was measured using a vernier microscope accurate to ± 0.01 mm (which corresponded to an actual distance of approx. ± 0.025 mm). Subsequently, the interferograms were interpreted using the relation between index of refraction and temperature data [25] to obtain the temperature profiles. The single reference temperature needed to interpret the interferograms was measured with a calibrated type-T thermocouple located 3.5 cm above the bottom plate. The estimated accuracy of the temperature measurement was about ± 0.1 C. A more detailed discussion of the data reduction procedure used can be found elsewhere [23].

2.2. *Analysis*

When an initially quiescent, thermally stratified fluid is heated from below a thin layer of warmer and therefore lighter fluid is created adjacent to the bottom by conduction of heat. As soon as the critical Rayleigh number has been exceeded, this layer breaks up into thermals ('mushroom' like convection elements) which penetrate the underlying stable layer. Through turbulent mixing the thermals produce a layer of fluid which is at a relatively uniform temperature. The dynamics of this layer, e.g. increase in its depth and mean temperature with time, under the imposed thermal conditions, is of considerable practical importance in the understanding, design and performance of many systems which are of geophysical and technological interest. The two-differential equation (e.g. for the turbulent kinetic energy k and the turbulent kinetic energy dissipation ε) model of turbulence [26] was used in conjunction with the unsteady, 1-dim. (horizontal advection is negligible) conservation equations of momentum and energy [27] to predict the unsteady

temperature distribution in the mixed layer and the stable region above. Based on the flow visualization using a shadowgraph and the interference fringe patterns reported, the 1-dim. assumption appears to be a good approximation.

If all thermophysical properties (except the density in the buoyancy force term) are temperature independent and the Boussinesq approximation is assumed valid, the 1-dim. conservation equations for momentum and energy transport reduce to

$$\rho\frac{\partial u}{\partial t} = -\frac{\partial p}{\partial x} + \frac{\partial}{\partial z}\left[(\mu + \mu_t)\frac{\partial u}{\partial z}\right] \quad (1)$$

$$\rho\frac{\partial v}{\partial t} = -\frac{\partial p}{\partial y} + \frac{\partial}{\partial z}\left[(\mu + \mu_t)\frac{\partial v}{\partial z}\right], \quad (2)$$

and

$$\rho c\frac{\partial T}{\partial t} = \frac{\partial}{\partial z}\left[(k + k_t)\frac{\partial T}{\partial z}\right] - \frac{\partial F}{\partial z}. \quad (3)$$

The models for predicting the turbulent viscosity, μ_t, and the turbulent thermal conductivity, k_t, are presented below. The radiation flux divergence $\partial F/\partial Z$ is included here for generality since stratification by radiation is not modeled.

The initial conditions for an initially stagnant layer of water are assumed to be

$$T(z,0) = T_0(z) \quad (4)$$

and

$$u(z) = v(z) = 0. \quad (5)$$

The boundary conditions for a layer of water with a free surface (i.e. air–water interface) can be expressed as

$$k_{\text{eff}}\frac{\partial T}{\partial z}\bigg|_{z=0} = q_b \quad \text{or} \quad T = T_b \quad (6)$$

and

$$u = v = 0 \quad (7)$$

at the bottom $z = 0$ and

$$k_{\text{eff}}\frac{\partial T}{\partial z}\bigg|_{z=D} = q_s = q_{\text{conv}} + q_{\text{lat}} + q_{\text{rad}} \quad (8)$$

as well as

$$u = v = 0 \quad (9)$$

at the free surface $z = D$.

The turbulent viscosity, μ_t, is calculated using the k–ε model of turbulence [26]. The equations for the turbulent kinetic energy k and turbulent kinetic energy dissipation ε are

$$\rho\frac{\partial k}{\partial t} = \frac{\partial}{\partial z}\left[\left(\frac{\mu_{\text{eff}}}{Pr_k}\right)\frac{\partial k}{\partial z}\right] + \mu_t\left[\left(\frac{\partial u}{\partial z}\right)^2 + \left(\frac{\partial v}{\partial z}\right)^2\right] + \frac{\mu_t g\beta}{Pr_t}\frac{\partial T}{\partial z} - \rho\varepsilon \quad (10)$$

and

$$\rho\frac{\partial \varepsilon}{\partial t} = \frac{\partial}{\partial z}\left[\left(\frac{\mu_{\text{eff}}}{Pr_\varepsilon}\right)\frac{\partial \varepsilon}{\partial z}\right] + C_{1\varepsilon}\mu_t\left(\frac{\varepsilon}{k}\right)\left[\left(\frac{\partial u}{\partial z}\right)^2 + \left(\frac{\partial v}{\partial z}\right)^2\right] - C_{3\varepsilon}\mu_t\left(\frac{\varepsilon}{k}\right)\left(\frac{g\beta}{Pr_t}\right)\frac{\partial T}{\partial z} - C_{2\varepsilon}\rho\left(\frac{\varepsilon^2}{k}\right). \quad (11)$$

Constants and parameters in equations (10) and (11) are from the literature [26, 27]. In terms of k and ε, the turbulent viscosity, μ_t, can be expressed as

$$\mu_t = C_\mu\rho k^2/\varepsilon. \quad (12)$$

The initial conditions for the turbulence model are evaluated by assuming that the initial level of turbulence is negligible in the water and can be represented as

$$\mu_t(z,0) = 0 \quad (13)$$

and

$$k(z,0) = \varepsilon(z,0) = 0. \quad (14)$$

The momentum, energy and turbulence equations were solved numerically using the GENMIX computer program for 2-dim. parabolic partial differential equations [28].

2.3. *Results and discussion*

2.3.1. *Qualitative discussion of observed phenomena.* A number of experiments in which the initial water temperature varied almost linearly and nonlinearly have been performed but only one experiment (experiment 1) is discussed here for the sake of brevity and also because the physical processes which can be inferred from the interferograms are very similar for different initial thermal stratifications. In this particular experiment the initial temperature increased almost linearly with the distance from the cell bottom. Two photographs illustrating interference fringe patterns are shown in Fig. 2. The reference thermocouple seen in the photographs was located about 3.5 cm from the bottom. The photographs show the entire fluid layer and indicate that the free surface of the water is effectively insulated, because a thin, nearly uniform temperature layer exists just below the surface. Examination of the interferograms recorded earlier ($t < 30$ s) showed that the distance between the bottom few fringes increased, but they remained parallel indicating purely conductive heat transfer. Since the bottom plate was warmer than the fluid immediately above it, conduction of heat into the water produced a temperature reversal in the water just above the plate. After about 45 s from the start of circulation of warm fluid through the passage, the bottom few fringes started to become wavy and moved very rapidly away from the plate. This indicated the onset of natural convection. After the onset of convection (i.e. Rayleigh number exceeding a critical value), the fluid layer adjacent to the plate became unstable and thermals broke away from the surface and plunged into the thermally stratified stable layer above (see Fig. 2a). The figure shows that the breaking away of thermals from

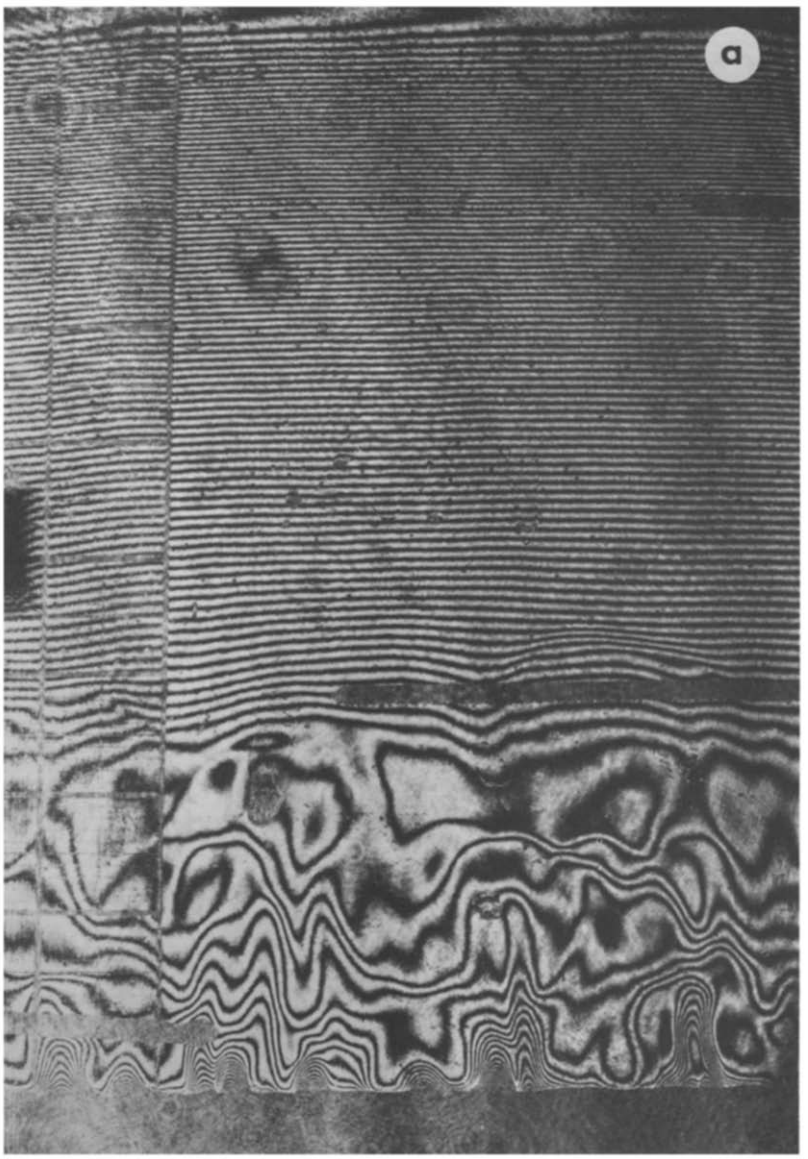

FIG. 2(a). Photograph of interference fringe patterns for experiment 1, $D = 9.56$ cm, $T_f = 27.0$ C, $T_{bo} = 17.1$ C and $t = 2$ min.

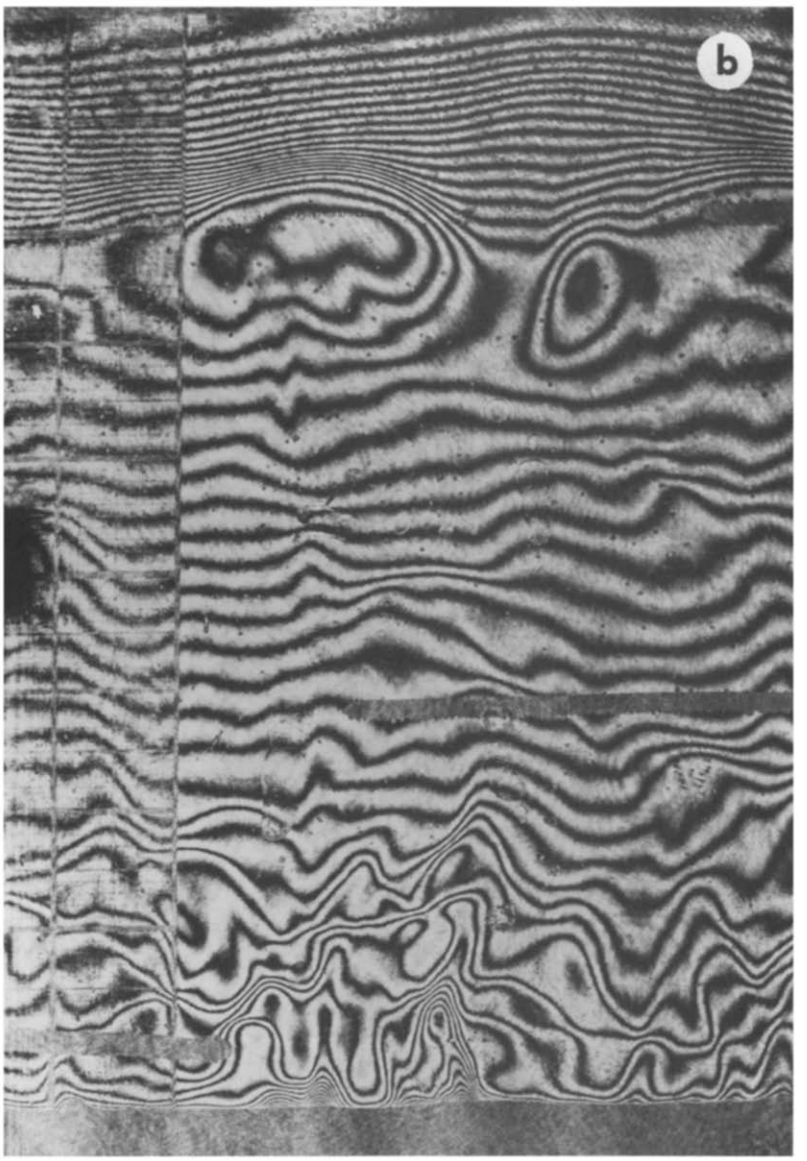

FIG. 2(b). Photograph of interference fringe patterns for experiment 1, $D = 9.56$ cm, $T_i = 27.0$°C, $T_{bo} = 17.1$°C and $t = 8$ min.

the plate creates mixing and agitation which in turn creates a relatively uniform temperature ('mixed') layer of water which is about 2 cm deep.

The generation of the thermals are due to the instability created in the layer adjacent to the heated surface. This is clearly evident from Fig. 2(a) which shows that the thermals are at a temperature different from that of the bottom plate. The start of the ascending warm water appeared at random locations and no characteristic wavelength (wavenumber) could be defined for the process (see Figs. 2a and 2b). The temperature of the thermals was not uniform across it and there was a considerable temperature difference (1°C) between the center and the outer edge of thermals. The voltage output of the thermistor located a few millimeters above the plate indicated that the upward moving thermals were approx. 0.4–2.0 C warmer than the surrounding bulk mean temperature.

As the ascending thermals reach the stratified region, a parcel of this warmer fluid plunges into it and disturbs the interface between the mixed and stratified layers. As a result of this bombardment, the warmer fluid in the stable region is entrained into the mixed layer, and the layer grows at the expense of erosion of the bottom of the stratified fluid. The fringes at the bottom of the stratified region became wavy and distorted owing to the bombardment of the interface by the thermals which plunge into the stable region before spreading along the interfacial layer. Shadowgraph images which were photographed by blocking the test beam in the reference leg of the inferometer provide clearer evidence than the interference patterns that the flow is 3-dim., i.e. the thermals generated are not plane perpendicular to the test beam. The photographs clearly indicate that as a thermal rises through the relatively quiescent fluid environment, its leading edge is blunted and folded back, producing a nearly hemispherical cap and giving a mushroom-like appearance to the thermal as a whole.

2.3.2. *Comparison of predictions with data.* Before proceeding to the predictions based on the k–ε model with the experimental data, it should be mentioned that the empirical model constants were established using data from one of the experiments described by Deardorff *et al.* [8], and no adjustments in these constants were made when predicting the temperature distribution for the experiments described in this paper. The values of the constants, with the exception of $C_{3\varepsilon}$ as recommended by Launder and Spalding [26] were used. $C_{3\varepsilon} = 0.8$ yielded best agreement with Deardorff's *et al.* data and was therefore used throughout the calculations. However, it should be emphasized that the empirical constants C_μ, $C_{1\varepsilon}$, $C_{2\varepsilon}$ and $C_{3\varepsilon}$ have not been as firmly established for buoyancy than for shear dominated flows [29]. It is suffice to note that 40 nodes were used in the numerical calculations. The computational details can be found elsewhere [23].

Comparisons between the measured and predicted

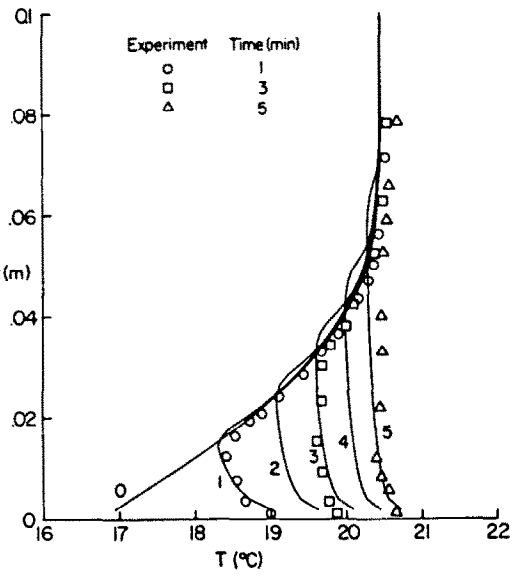

FIG. 3. Comparison between measured and predicted temperature distributions in the bottom mixed layer during heating from below for experiment 2, $D = 14.8$ cm, $T_f = 21.9$°C, $T_{b0} = 16.8$°C.

temperature distributions for experiments 2 and 3 with different initial temperature profiles are shown in Figs. 3 and 4, respectively. For reasons of clarity, data points are purposely not shown at all the times for which the temperature profiles are calculated. The agreement between data and analysis is very good for all times (Fig. 3). In this particular experiment a relatively uniform layer of water was seen to overlay the stratified layer. The experimental results show that the temperature of this uniform layer of water ($z > 6$ cm) increases slowly as the heating continues. However, the model predicts no change in the temperature of this layer. This discrepancy may, in part, be due to the modeling of the air–water interface as being insulated. Within the first few millimeters of the bottom analysis over-

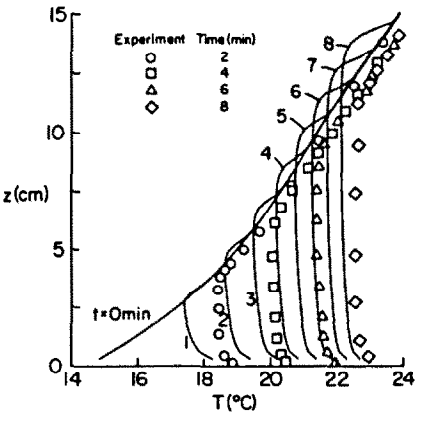

FIG. 4. Comparison between measured and predicted temperature distributions in the bottom mixed layer during heating from below for experiment 4, $D = 14.6$ cm, $T_f = 25.4$°C, $T_{b0} = 14.6$°C.

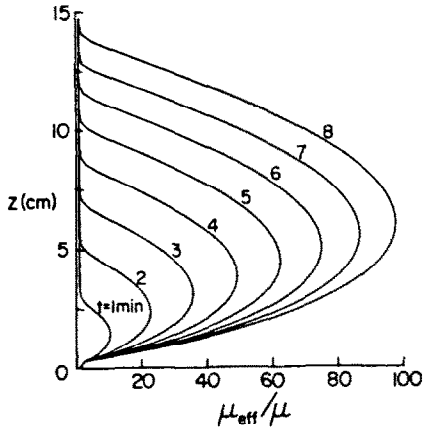

FIG. 5. Predicted dimensionless effective velocity profiles for experiment 4 (see Fig. 4 for conditions).

predicts the temperature. This appears to be the consequence of inadequate modeling of turbulence near the solid boundary, particularly in the thin 'conduction' layer a few millimeters in thickness located above the heated bottom. When the fluid is more intensely stratified initially (Fig. 4) the model predicts a clear 'overshoot' right above the mixed layer. The overshoot was not observed interferometrically because of the averaging of temperature along the test beam; however, other investigators [8] using thermocouples for measuring temperature have observed and discussed the overshoot. The predictions show that the magnitude of the overshoot increases as the heating continues.

The reason the temperature in the mixed layer is rather uniform is because the effective viscosity, μ_{eff} (Fig. 5), and the effective conductivity, k_{eff}, over an order of magnitude larger than the molecular viscosity, μ. The reasonably good agreement between data and predictions suggest that the predicted effective viscosities model the general trends and relative order of magnitude of turbulence at different times as the heating continues. As is clearly evident from the figure, the peaks in the μ_{eff} profiles move upward with time. This is due to the growth of the mixed layer. The upward heat flux decreases with depth z, resulting in a small potential for turbulence driving force at larger z. As a result there is a sharp increase in the viscosity near the bottom of the layer and the peak is shifted down. The results presented here, and those available elsewhere [23], show that the initial temperature distribution (i.e. intensity of stratification) and the heat input into the mixed layer at the bottom are important factors controlling the mixed layer temperature, mixed layer dynamics and level of turbulence in buoyancy-driven flows.

A comparison between measured data for two experiments and predictions for mixed layer depth and temperature is presented in Fig. 6. The agreement between experimental data and the model for both the mixed layer depth and temperature is good for all experiments. The predictions are consistently higher for both the mixed layer depth and temperature at early times and also somewhat higher at later times. This is due to the fact that early in the experiments the turbulence is not yet fully developed, and therefore the model overpredicts the mixed layer height and temperature. Also, at early times the model yielded a relatively rapid growth rate for both the dissipation and production terms of the turbulent kinetic energy, and therefore resulted in overprediction of both the temperature and the depth of the mixed layer.

The relatively rapid initial growth of the dissipation term in the model equations results in a decrease of the total internal energy of the mixed layer which in turn causes a decrease in the time rate of change of the mixed layer temperature predicted by the model. As a consequence, this results in underprediction of the mixed layer temperature at later times. As discussed earlier, the values of the constants in the model used were established in accordance with the experimental results of Deardorff *et al.* [8]. However, their experiments were performed in a system with uniform initial stratification of water while in the present study the stratification of water was not uniform. Use of the constants based on an experiment with uniform stratification may partially account for the discrepancy between the model predictions and data.

3. COOLING OF THERMALLY STRATIFIED WATER FROM ABOVE

3.1. *Experiments*

3.1.1. *Test apparatus.* The experimental apparatus for simulating the cooling of thermally stratified water from above is shown in Fig. 7. The apparatus consisted of a cell with an air channel above it to model cooling and wind shear at the water surface. Solar radiation was simulated using high temperature tungsten filament lamps in parabolic reflectors of known spectral radiative characteristics.

The test cell used in the experiments was designed for photographic and optical observations of flow and mixing processes. The cell was 33 cm deep, 25 cm long and 10 cm wide. Two sides of the cell were 45 × 30 cm in size and were of 2.5 cm thick higher-quality optical glass. The other sides and the bottom were of 2.5 cm thick Plexiglas. The sides and bottom of the test cell were milled together to 10 cm ($\pm$0.0015 cm) to insure a uniform cell width. A layer of removable 5 cm thick styrofoam insulation covered the faces and sides of the tank.

A channel for inducing air flow over the water surface was designed as part of the cell and installed on its top. To ensure a smooth transition of air flow over the water surface and to enable observation, the optical sides were also the sides of the air channel. This channel consisted of five sections: an entrance with flow straighteners, a working length, a fan entrance with flow straighteners, a fan duct, and a fan. The cross section of the air channel was 10 × 10 cm and the total

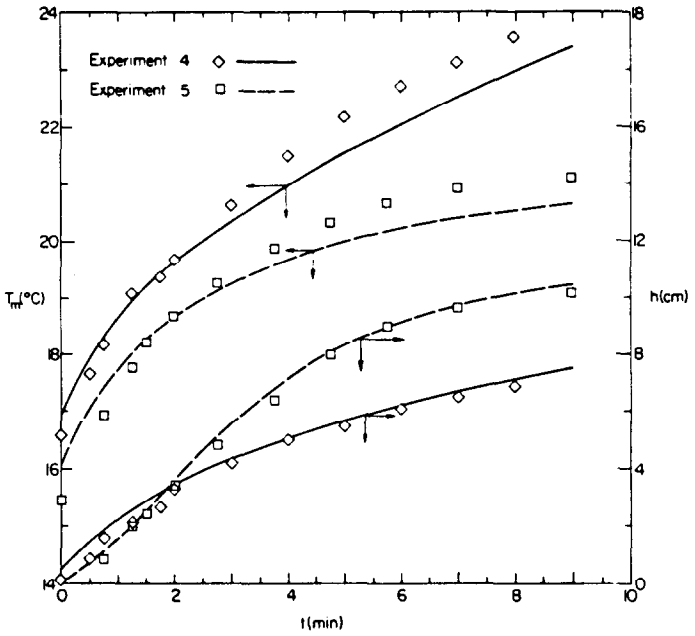

FIG. 6. Comparison between measured and predicted mixed layer heights and mean temperatures for experiment 1 (see Fig. 4 for conditions) and experiment 2 with D = 13.4 cm, T_f = 24.7°C, T_{b0} = 21.7°C.

length of the channel was about 2 m. The top wall of the wind channel above the water surface was of clear float glass. A much larger test cell and air channel, e.g. of the size used by other investigators [18, 20], would have been desirable. Unfortunately, the need to uniformly irradiate a large surface of water and the choice of optical diagnostics for visualizing the flow field made the usage of such a cell impossible.

Solar radiant heating of water was simulated using two tungsten filament lamps with parabolic reflectors which were described in the previous section. The spectral transmission characteristics of transparent (glass) covers forming the top of the wind channel were measured. The spectral characteristics of the radiant heaters (with the tungsten filament operating at temperatures between 2800 and 3250 K) were known, and the total radiation flux incident on the water surface was measured with a radiometer.

The instrumented test cell was placed in one leg of a Mach–Zehnder interferometer which was already described. Because the interferometer could not accommodate the entire lower part of the test cell, numerous thermocouples (including those used for references) were installed in it. In the lower part of the cell, temperature measurements were made with thermocouples only. Before and after each experiment the distance between a reference thermocouple was measured with a cathetometer.

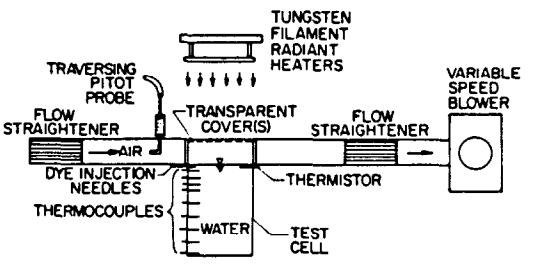

FIG. 7. Schematic diagram of test apparatus.

A calibrated thermistor with a 2 mm dia. bead (installed about 1 cm below the surface) was used to detect temperature fluctuations. This thermistor was carefully calibrated. A traversing Pitot-type probe was used to measure the stagnation and total pressure of air with a micromanometer with a minimum resolution of ± 0.0025 mm of fluid (n-butyl alcohol) and an estimated accuracy of about ± 0.005 mm.

Attempts to use a hot-film anemometer (DISA, Model 55M) system with a temperature compensator bridge and a hot-film dual probe to measure velocity of water were unsuccessful. At low velocities (<0.2 cm s^{-1}) the anemometer was not sufficiently sensitive and, also, the free convection velocities induced by heating of the probe were of the same order of magnitude as the imposed forced flow velocities during calibration. Therefore, flow visualization methods had to be employed [31]. Flow of water in the test cell was visualized using black–blue dye, 'fish-scales' particle tracing, and shadowgraphic methods. The details of the experimental procedures and results are given elsewhere [31].

3.1.2. *Test procedure.* The test cell was cleaned, flushed and filled with distilled and deionized water, covered and left undisturbed for some time to eliminate all convection currents which are normally present and allowed to attain a uniform temperature equal to that of the surroundings. After it had been determined that

all the convection motions in the tank were settled out, the interferometer was adjusted to an infinite fringe. The water in the tank was thermally stratified by irradiation of its surface from the radiant heaters located above the test cell. After the desired thermal stratification condition was reached two different types of experiments were performed: (1) the radiant heating was terminated and the water surface was cooled by forcing ambient room temperature air over the surface, or (2) the radiant heating was continued and the cooling of the water surface was initiated.

The interference fringe patterns at prescribed time intervals were photographed (by quickly removing the removable insulation and then immediately replacing) with a 35 mm camera. The fringe data were reduced in the same manner as described in the previous section. The air velocity profiles in the air channel were measured using a traversing Pitot-type static probe and a static top. The probe had been previously callibrated for different blower speed settings.

3.2. *Analysis*

A detailed discussion of the internal transport processes in waters and interactions at a water surface have been presented [22], and thus only a physical-mathematical model is detailed. Based on flow visualization results obtained, it is assumed that energy transport in the water is 1-dim. (horizontal advection is neglected) and the mean velocity in the vertical direction is negligible in comparison to the horizontal components. Internal waves, natural currents, and Coriolis forces are also neglected. It is further assumed that there is no variation in the horizontal distribution of heat and momentum fluxes at the air water interface and that all physical properties (except for the density in the buoyancy force) are temperature independent and the Boussinesq approximation is valid.

Based on the above idealizations, the identical equations to those given in the previous section, equations (1)-(3), were used. The analysis for predicting the local radiation flux F and its divergence $\partial F/\partial z$ is detailed elsewhere [32]. Suffice it to say that the radiation incident on the water surface was resolved into diffuse and beam components and a forward scattering approximation was employed to solve the 1-dim. radiative transfer equation. The air-water interface was considered as optically smooth, and the radiation characteristics were predicted from Fresnel's equations. The bottom was assumed to be a diffuse reflector. Calculations were performed on a spectral basis using the spectral absorption coefficient of distilled water.

The initial conditions before the start of the radiant heating are identical to those given by equations (4) and (5). With the coordinate origin at the water surface, conditions at the air-water interface ('s') are given by

$$\tau_{sx} = (\mu + \mu_t)\frac{\partial u}{\partial z}\bigg|_{z=0} \tag{15}$$

$$\tau_{sy} = (\mu + \mu_t)\frac{\partial v}{\partial z}\bigg|_{z=0} \tag{16}$$

$$-k\frac{\partial T}{\partial z}\bigg|_{z=0} = q_s = q_{conv} + q_{lat} + q_{rad}. \tag{17}$$

Heat transfer at the air-water interface is by convection, latent energy transport, and long-wave length radiation. Empirical relations have been used to predict momentum and energy transport at the interface [23]. At the bottom of the layer ($z = D$) the boundary conditions are

$$u = v = 0 \tag{18}$$

$$k\frac{\partial T}{\partial z}\bigg|_{z=D} = \int_0^\infty \alpha_{b\lambda} F_\lambda(z = D)\,d\lambda. \tag{19}$$

Equation (19) states that the bottom is insulated and absorption of radiation is balanced by heat conduction into the water.

The turbulence model is identical to that described in Section 2.2. The momentum, energy and turbulence equations were solved numerically using the GENMIX computer code [28] for 2-dim. parabolic partial differential equations. The empirical correlations used to determine the convective heat and mass transfer coefficients are given elsewhere [23].

3.3. *Results and discussion*

3.3.1. *Flow visualization.* A number of flow visualization experiments which have been performed are described elsewhere [31] and need not be repeated here. Suffice it to note that the results obtained using blue-black dye and fish-scales tracer visualization methods show that the flow in a thermally stratified layer of water cooled from above by air flow over the free surface is confined and mixing occurs only in the upper surface layer. Flow visualization experiments performed showed that when thermally stratified water (by radiant heating) is cooled from the surface, a mixed layer of nearly uniform depth along the cell developed. As the cooling continued the layer grew in depth at the expense of the underlying stratified region below. The stable stratification in the underlying layer resisted and confined the flow. The entrainment of warmer water from the stable region into the mixed layer contorted the interface between the convective and stable layers. Parcels of warmer water penetrated the underlying layer and bombarded the interface. Photographs of the shadowgraph and Mach-Zehnder interferometer images (also the thermistor output) confirmed the small scale circulation patterns and plume activities in the mixed layer. Circulation in the mixed layer was also evidenced by the alignment of tracer particles (fish-scales) with the roll patterns. The small scale circulation patterns and plume activity were also confirmed by the output of a thermistor which was located about 1 cm below the free surface.

A typical photograph of the interference fringe patterns recorded during one experiment is illustrated in Fig. 8. The photograph shows only about the upper

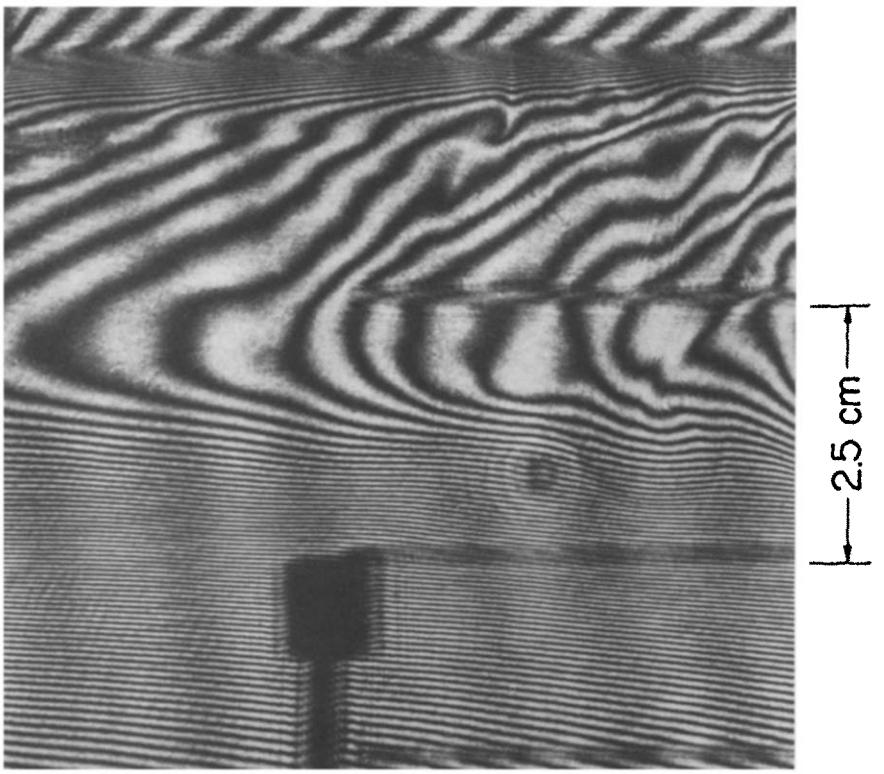

FIG. 8. Photographs of interference fringe patterns during cooling of thermally stratified (by first irradiating layer of water at $T_0 = 21.0$°C with $F_{inc} = 2370$ W m^{-2} for 30 min) water, $T_a = 27.1$°C, $V_a = 4.8$ m s^{-1}, $\phi = 61°_{00}$, $t = 55$ min.

quarter of the water layer. The fringe patterns shown provide clear evidence of temperature reversal a small distance below the surface, indicating that the interface is being cooled. Due to evaporation of water from the surface and condensation on the glass the air water interface cannot be clearly identified in the photograph. The diagonal fringes at the top of the photograph indicate a temperature gradient in the air above the surface. Just below the surface there existed a surface boundary layer a few millimeters thick in which the temperature increased with depth. In this region the closely spaced fringes indicate the existence of large temperature gradients, and the fact that the fringes are nearly parallel provides evidence that in this thin

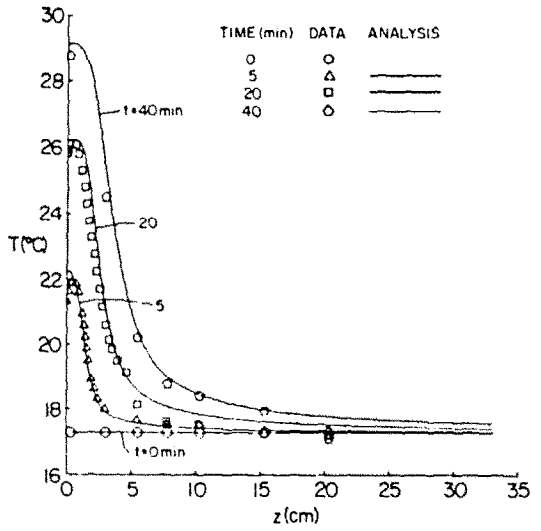

FIG. 9. Comparison between measured and predicted temperature distributions during the cooling phase of experiment B (see Fig. 8 for conditions).

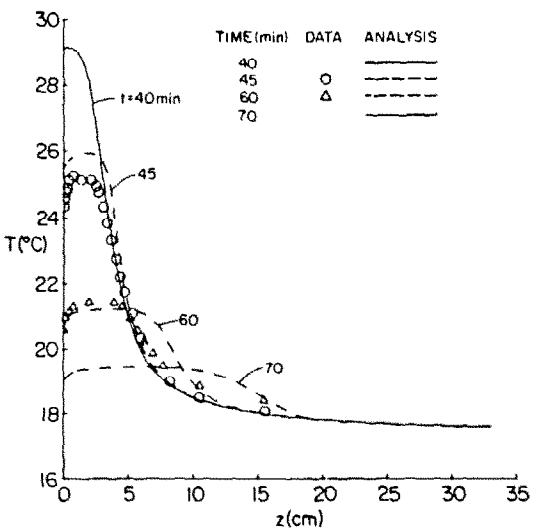

FIG. 10. Comparison of measured and predicted mixed layer depths (h) and mixed layer temperature (T_m) the depth of 3 mm for experiment B (see Fig. 8 for conditions).

boundary layer heat transfer is predominantly by molecular diffusion. Below the boundary layer lies a relatively uniform temperature mixed layer whose thickness grows with time. Mixing in this layer is primarily induced by buoyancy forces in the water and mechanical shear stresses at the surface. The flow structure in this layer was initially in the form of rolls which later broke into an irregular motion (Fig. 8). A similar flow structure was observed during the cooling from above of a thermally stratified water in the absence of forced air flow over the surface [33].

3.3.2. *Comparison of experimental data with predictions.* A comparison between model predictions and data for experiment B is given in Figs. 9 and 10. In this particular experiment the water was heated by radiation and simultaneously cooled by forced air flow over the surface. Figure 9 gives a comparison of the measured and predicted temperature distributions during this cycle. Because of the intense stratification (at $t = 40$ min) and the high fringe density, the interferograms could not be interpreted, and thus the temperature profile at this time was measured with thermocouples. The good agreement between the experiment and analysis during stratification of water by radiation confirms the reliability and accuracy of the radiation model for laboratory experiments with distilled water.

A comparison between predicted and measured temperature distributions during the cooling phase of the experiment (with radiant heaters turned off) shown in Fig. 10 reveals good agreement; however, the mixed layer temperature at $t = 45$ min is overestimated, while at $t = 60$ min it is slightly underestimated. The model overpredicts the depth of the mixed layer. The discrepancy between the data and predictions in the temperature distribution and the depth of the mixed layer is attributed to inadequate modeling of the sensible and latent heat transfer at the water surface and the entrainment process between the mixed and the stably stratified regions. With cooling and application of wind shear at the water surface, the effective viscosities calculated [23] show that the turbulence intensifies and that μ_{eff}/μ reaches a maximum value of about 28 at $t = 70$ min.

The results of calculations have shown that in the presence of wind shear at the surface, even for a thermally stratified layer of water, the production of turbulence term in the k-equation, equation (10) (second term on the RHS of the equation), is the most important term. This term is nearly balanced out, mainly by the dissipation of turbulent kinetic energy term ε. The diffusion of turbulent kinetic energy and the production of turbulent kinetic energy by density (temperature) gradient terms are relatively unimportant. The buoyancy term in the k-equation is positive near the surface which implies production and then becomes negative away from the interface indicating dissipation. In the ε-equation, equation (11), the production term (second term on the RHS of the equation) is also the most important one which is nearly balanced out by the dissipation term (last term on the RHS of the equation). The diffusion of dissipation of turbulent kinetic energy is significant only near the interface. The effect of buoyancy in the k-equation is more pronounced than in the ε-equation. The negative temperature gradient away from the interface, which corresponds to thermally stable stratification, retards the development of turbulence in this region. This is in agreement with the experimental observations discussed previously.

The temperature distribution in the water depends strongly on surface boundary conditions and turbulence in the mixed layer. The overall validity of the model prediction is examined in Fig. 11 where the calculated mixed layer depth and temperature are compared with the measurements. Good agreement is obtained between the calculated and measured mixed layer depth. Since it was impossible to determine the surface temperature accurately (due to the large interference fringe density), the temperature measured with a thermocouple 3 mm below the interface was used for comparison.

A comparison between the predicted and measured temperature profiles for experiment C is shown in Fig. 12. In this particular experiment an initially stagnant layer of water was first stratified thermally by radiant heating for 30 min. Then heating was discontinued and the water cooled by forced air flow over the surface from $t = 30$ min to $t = 60$ min. At $t = 60$ min the radiant heating of the water was restarted and continued for 30 min until the test was terminated. The purpose of the experiment was to model the insulation and cooling processes of natural waters.

The results of Fig. 12 show that during the cooling phase the model overpredicts the depth and temperature of the mixed layer. The discrepancy is partially due to inadequate modeling of turbulence and of the heat transfer processes at the air–water interface. At $t = 45$ min the calculated total thermal energy content of water is higher than that measured experimentally. This suggests that the model equations underpredicted the surface heat flux. The experimental and numerical results indicate that the temperature distribution at depths greater than 15 cm change little during the

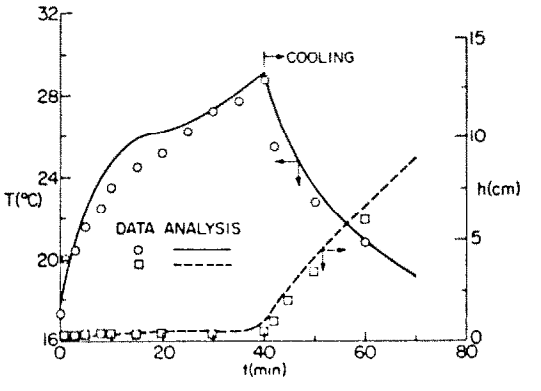

FIG. 11. Comparison of measured and predicted mixed layer depth and temperature for experiment B.

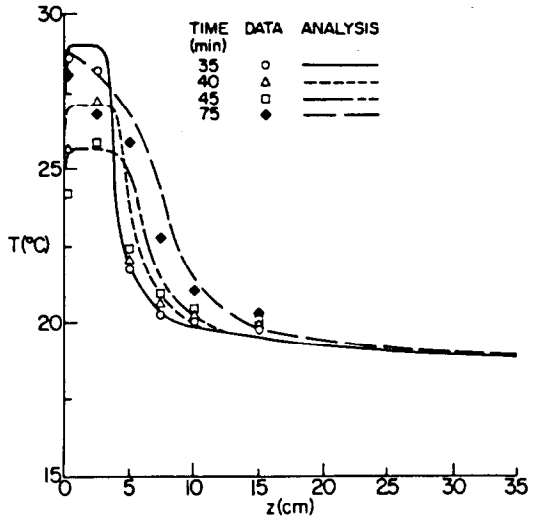

FIG. 12. Comparison of measured and predicted temperature distributions during the cooling ($30 < t < 60$ min) and reheating ($60 < t < 90$ min) phases for experiment C, $T_0 = 17.3$°C, $T_a = 18.9$°C, $V_a = 4.8\ m\ s^{-1}$, $\phi = 64\%$ and $F_{inc} = 2030\ W\ m^{-2}$.

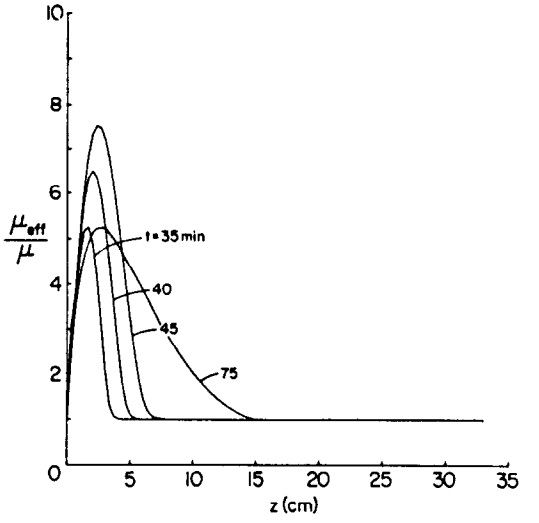

FIG. 13. Predicted effective viscosity distributions for conditions of experiment C (see Fig. 12 for conditions).

experiment. The calculated temperature distributions during the restratification (simultaneous radiant heating and cooling) phase of the experiment ($t = 75$ min) suggest, that the model is capable of fair predictions. The calculated effective viscosity profiles are illustrated in Fig. 13 and show that at $t = 75$ min the peak value of the effective viscosity is 30% lower than at $t = 45$ min. This is due to suppression of turbulence by deposition of radiant energy in water during restratification. Although at this time the turbulence level is lower, the mixed layer deepens as a result of surface cooling and turbulent entrainment of water from the stable region.

4. CONCLUSIONS

The temperature distributions, mixed layer heights, and mean temperatures predicted with the 1-dim. model in conjunction with the $k-\varepsilon$ differential equation model of turbulence agreed well with the experimental data. The discrepancy between predictions and data is attributed to the uncertainty in the turbulence model constants and their dependence on stratification conditions. The entrainment processes in the interfacial region between the mixed layer and the overlaying stable region above it do not appear to be modelled adequately.

The flow in a thermally stratified layer of water cooled by air flow over the surface is confined and mixing occurs only in the upper region, but the stable region erroded as the cooling continued. Internal absorption of radiation plays an important role in the flow and the thermal structures in water simultaneously heated by radiation from an external source and cooled by forced air flow over the surface. The interaction of radiation and turbulent mixing in a layer of water which is cooled from the surface has important bearing on the mixed layer dynamics. The $k-\varepsilon$ model of turbulence is not completely satisfactory for predicting the temperature structure and the dynamics of the mixed layer during simultaneous radiant heating and cooling or during cooling of thermally stratified water. There is uncertainty in the model parameters for buoyancy and shear driven mixing, and the entrainment processes in the interfacial layer between the mixed and stable regions do not appear to have been modeled adequately.

Acknowledgements—The authors wish to acknowledge fruitful discussions with Professor D. B. Spalding regarding modeling of turbulence and use of the GENMIX computer program. The work on which this paper is based was supported in part by funds provided by the Office of Water Research and Technology (matching grant project No. OWRT-B-077-IND), U.S. Department of Interior, Washington, U.S.A., as authorized by the Water Research and Development Act of 1978 through the Water Resources Research Center of Purdue University.

REFERENCES

1. Z. Zaric, Editor, *Thermal Effluent Disposal from Power Generation*. Hemisphere, Washington (1977).
2. S. B. Savage, Solar Pond, in *Solar Energy Engineering*, pp. 217–232 (edited by A. A. M. Sayigh). Academic Press, New York (1977).
3. J. Straub, G. Merker, K. Kuhlbeck, A. Staudt and U. Grigull, Untersuchung der Konvektion in Jahreswärmespeichern, *VDI-Ber.* **288**, 39–46 (1977).
4. D. B. Spalding and N. Afgan, Editors, *Heat Transfer and Turbulent Buoyant Convection: Studies and Applications for Natural Environment, Buildings, and Engineering Systems*, Vols. 1 and 2. Hemisphere, Washington (1977).
5. C. E. Nielsen, Non-convective salt gradient solar ponds, in *Solar Energy Technology Handbook*, Part A, pp. 345–376 (edited by W. C. Dickinson and P. N. Cheremisinoff). Marcel Decker, New York (1979).
6. H. Tabor, Solar ponds, *Sol. Energy* **27**, 181–194 (1981).
7. H. J. Leyers, F. Scholz and A. Tholen, Analytical and

experimental determination of the temperature distribution in stratified hot water stores, in *Energy Conservation in Heating, Cooling and Ventilating Buildings*, pp. 683–693 (edited by C. J. Hoogendoorn and N. H. Afgan). Hemisphere, Washington (1978).
8. W. J. Deardorff, G. E. Willis and D. K. Lilly, Laboratory investigation of nonsteady penetrative convection, *J. Fluid Mech.* **35**, 7–31 (1969).
9. F. D. Heidt, Comparison of experiments on penetrative convection with measurements in nature, in *Heat Transfer in Buoyant Turbulent Convection*, Vol. 1, pp. 199–210 (edited by D. B. Spalding and N. Afgan). Hemisphere, Washington (1977).
10. K. B. Katsaros, W. T. Lin, J. A. Businger and J. E. Tillman, Heat transport and thermal structure in the interfacial boundary layer measured in an open tank of water in turbulent free convection, *J. Fluid Mech.* **83**, 311–335 (1977).
11. J. S. Turner, *Buoyancy Effects in Fluids*. Cambridge University Press, Cambridge (1973).
12. D. M. Snider and R. Viskanta, Radiation induced thermal stratification in surface layers of stagnant water, *Trans. Am. Soc. Mech. Engrs*, Series C, *J. Heat Transfer* **97**, 35–40 (1975).
13. S. Bloss and U. Grigull, Temperaturverteilung in tiefen und flachen Seen, *Wärme- und Stoffübertragung* **11**, 119–130 (1978).
14. J. M. K. Dake and D. P. Harleman, Thermal stratification in lakes: Analytical and experimental studies, *Wat. Resour., Wash.* **5**, 484–495 (1969).
15. R. Viskanta, M. Behnia and A. Karalis, Interferometric observations of the temperature structure in water cooled or heated from above, *Adv. Wat. Resour.* **1**, 57–69 (1977).
16. L. R. Wyatt, The entrainment interface in a stratified fluid, *J. Fluid Mech.* **86**, 293–311 (1978).
17. R. W. Garwood, Jr., Air-sea interaction and dynamics of the surface mixed layer, *Rev. Geophys. Space Phys.* **17**, 1507–1524 (1979).
18. C. Y. Shaw and Y. Lee, Wind-induced turbulent heat and mass transfer over large bodies of water, *J. Fluid Mech.* **77**, 645–664 (1976).
19. A. I. Ginzburg and K. N. Federov, Cooling of water from the surface under free and forced conditions, *Atm. Ocean. Phys.* **14**, 57–62 (1978).
20. P. A. Mangarella, A. J. Chambers, R. L. Street and E. Y. Hsu, Laboratory studies of evaporative and energy transfer through a wavy air–water interface, *Phys. Ocean.* **3**, 93–101 (1973).
21. R. L. Street, Turbulent heat and mass transfer across a rough, air–water interface: A simple theory, *Int. J. Heat Mass Transfer* **22**, 885–899 (1979).
22. M. F. Coantic, Coupled energy transfer and transformation mechanisms across the ocean–atmosphere interface, in *Heat Transfer 1978* Vol. 6, pp. 73–108. National Research Council of Canada, Ottawa (1978).
23. M. Behnia, Laboratory study of thermal and flow structures in heated and or cooled layers of water, Ph.D. Thesis, Purdue University (1979).
24. W. Hauf and U. Grigull, Optical methods in heat transfer, in *Advances in Heat Transfer* Vol. 6, pp. 133–366 (edited by T. F. Irvine, Jr. and J. P. Hartnett). Academic Press, New York (1970).
25. L. W. Tilton and J. K. Taylor, Refractive index and dispersion of distilled water for visible radiation at temperatures 0 to tp 60°C, *J. Res. Nat. Bur. Stand.* **20**, 419–477 (1938).
26. B. E. Launder and D. B. Spalding, *Lectures in Mathematical Models of Turbulence*. Academic Press, New York (1972).
27. D. B. Spalding and U. Svensson, The development and erosion of the thermocline, in *Heat Transfer and Buoyant Turbulent Convection* Vol. 1, pp. 113–122 (edited by D. B. Spalding and N. A. Afgan). Hemisphere, Washington (1977).
28. D. B. Spalding, *GENMIX: a General Computer Program for Two-dimensional Parabolic Phenomena*. Pergamon Press, Oxford (1977).
29. W. Rodi, Turbulence models for environmental problems, in *Predictions for Turbulent Flows*, pp. 259–349 (edited by W. Kollmann). Hemisphere, Washington (1980).
30. W. Merzkirch, *Flow Visualization*. Academic Press, New York (1974).
31. M. Behnia and R. Viskanta, Natural convection flow visualization in irradiated water cooled by air flow over the surface, in *Natural Convection in Enclosures*, pp. 17–26 (edited by K. E. Torrance and I. Catton). ASME, New York (1980).
32. R. Viskanta and J. S. Toor, Absorption of solar radiation in ponds, *Sol. Energy* **21**, 17–25 (1978).
33. M. Behnia and R. Viskanta, Free convection in a thermally stratified water cooled from above, *Int. J. Heat Mass Transfer* **22**, 611–623 (1979).

ETUDE EXPERIMENTALE ET ANALYTIQUE DU TRANSFERT THERMIQUE ET DU MELANGE DANS DES ECOULEMENTS THERMIQUEMENT STRATIFIES

Résumé—On étudie la convection naturelle instationnaire dans une couche d'eau stratifiée, de profondeur finie et chauffée par le bas. Des expériences de laboratoire sont menées avec un interféromètre Mach–Zehnder pour mesurer la température et une technique des ombres pour la visualisation. Un modèle monodimensionnel en conjonction avec un modèle de turbulence k–ε est utilisé pour prédire la dynamique de la couche de mélange qui si développe quand la fluide thermiquement stratifié est chauffé par le bas. Un bon accord entre les mesures et les calculs a été obtenu. Les mécanismes d'entrainement à l'interface entre la couche de mélange et la région stable, et la turbulence à la couche interfaciale peuvent être mieux compris pour une modélisation plus réaliste de la convection naturelle turbulente dans des fluides non uniformément stratifiés. La convection naturelle et le mélange sont étudiés expérimentalement et théoriquement quand une couche stratifiée de liquides est refroidie par un écoulement d'air sur la surface libre, ou quand une couche de liquide est simultanément chauffée par une source radiative et refroidie par un écoulement d'air à la surface. Des mesures de températures utilisent un interféromètre Mach–Zehnder, des thermocouples et un thermistor. La structure d'écoulement du fluide est visualisée par des traceurs et par la technique des ombres. Un modèle monodimensionnel et non stationnaire est développé pour prévoir le champ de température dans l'eau irradiée par une source externe et refroidie en surface par l'air. Le mélange turbulent est calculé avec le modèle k–ε. Les résultats montrent que le rayonnement joue un rôle important. La profondeur de la couche de mélange est surévaluée par le modèle de turbulence parce qu'il ne simule par correctement le mécanisme d'entrainement dans la couche intermédiaire entre les régions mélangée et stable.

EXPERIMENTELLE UND ANALYTISCHE UNTERSUCHUNG DES WÄRMEÜBERGANGS UND DER DURCHMISCHUNG IN THERMISCH GESCHICHTETEN AUFTRIEBSSTRÖMUNGEN

Zusammenfassung—In einer von unten beheizten, ungleichförmig geschichteten Wasserschicht endlicher Tiefe wurde nicht-stationäre freie Konvektion untersucht. In den Experimenten wurden ein Mach-Zehnder-Interferometer zur Temperaturmessung und ein Schattenschlierenverfahren zum Sichtbarmachen der Strömung benutzt. Zur Beschreibung des dynamischen Verhaltens der Mischungsschicht, die sich entwickelt, wenn ein thermisch geschichtetes Fluid von unten beheizt wird, wird ein eindimensionales Modell in Verbindung mit einem Zwei-Gleichungs-k-ε-Turbulenzmodell benutzt. Dieses Modell lieferte gute Übereinstimmung mit den Meßwerten. Für eine noch realistischere Modellierung der turbulenten freien Konvektion in ungleichförmig geschichteten Fluiden muß jedoch noch mehr Einsicht in den Austauschvorgang an der Übergangsfläche zwischen Misch-Schicht und dem stabilen Gebiet, wie auch in die Turbulenz in der Grenzflächenschicht gewonnen werden. Wärmeübergang und Durchmischung bei nicht-stationärer freier Konvektion, die auftreten, wenn entweder eine thermisch geschichtete Flüssigkeitsschicht durch Luftströmung über die freie Oberfläche gekühlt wird oder wenn eine Flüssigkeitsschicht gleichzeitig durch äußere Strahlung beheizt und durch Luftströmung über die freie Oberfläche gekühlt wird, wurden sowohl experimentell wie analytisch untersucht. Die Temperaturen wurden mit einem Mach-Zehnder-Interferometer, mit Thermoelementen und mit einem Thermistor gemessen. Die Strömung in der Flüssigkeit wurde mit schwarzblauem Farbstoff und mit Fischschuppen als Indikatoren, wie auch durch Schattenschlierenverfahren sichtbar gemacht.

Zur Bestimmung des Temperaturverlaufs in Wasser, das einer äußeren Strahlungsquelle ausgesetzt ist und gleichzeitig durch eine Luftströmung über die Oberfläche gekühlt wird, wurde ein nicht-stationäres eindimensionales Modell entwickelt. Die turbulente Durchmischung wurde mittels des k-ε-Turbulenz-Modells berechnet. Die Ergebnisse zeigten, daß bei gleichzeitiger Beheizung durch Strahlung und Kühlung durch Konvektion die Strahlungsaufnahme in Wasser bei durch Auftrieb- und Windschubspannung bedingten Mischvorgängen in Oberflächenschichten eine wichtige Rolle spielt. Das Turbulenz-Modell lieferte für die Tiefe der Mischungsschicht zu große Werte, weil es den Austauschvorgang in der Übergangsfläche zwischen den durchmischten und stabilen Gebieten nicht angemessen wiedergibt.

ЭКСПЕРИМЕНТАЛЬНОЕ И АНАЛИТИЧЕСКОЕ ИССЛЕДОВАНИЕ ТЕПЛОПЕРЕНОСА И ПЕРЕМЕШИВАНИЯ ТЕРМИЧЕСКИ СТРАТИФИЦИРОВАННЫХ ПОДЪЕМНЫХ ПОТОКОВ

Аннотация — Исследована нестационарная естественная конвекция в неоднородно стратифицированном нагреваемом снизу слое воды конечной толщины. Измерения температуры проводились с помощью интерферометра Маха-Цендера, а течение визуализировалось теневым методом. Расчет динамики слоя смешения, образующегося при нагревании снизу термически стратифицированной жидкости проводился по одномерной модели и модели турбулентности $k-\varepsilon$, состоящей из двух дифференциальных уравнений. Получено хорошее совпадение между экспериментальными данными и результатами расчетов. Однако, для построения более реалистической модели турбулентной естественной конвекции в неоднородно стратифицированных жидкостях необходимо лучшее понимание гидродинамических процессов на границе между слоем смешения и устойчивой областью, а также исследование характеристик турбулентности в промежуточном слое.

Аналитически и экспериментально исследовались теплоперенос при нестационарной естественной конвекции и процесс смешения в случае охлаждения термически стратифицированного слоя жидкости потоком воздуха над свободной поверхностью, а также в случае одновременного нагревания слоя внешним источником излучения и его охлаждения потоком воздуха по свободной поверхности. Температура измерялась интерферометром Маха-Цендера, термопарами и термистором. Структура потока визуализировалась внесением в жидкость темносиней краски и рыбьей чешуи, а также теневым методом. Разработана нестационарная одномерная модель для расчета температурного поля в слое воды, обогреваемом внешним источником излучения и одновременно охлаждаемом потоком воздуха вдоль свободной поверхности. Турбулентное смешение рассчитывалось с помощью модели турбулентности $k-\varepsilon$. Полученные результаты показывают, что присутствие излучения сильно влияет на подъемное и обусловленное ветром сдвиговое течения, вызванные процессами перемешивания в поверхностных слоях воды при одновременном нагреве излучением и охлаждении конвекцией. При использовании модели турбулентности получаются завышенные значения глубины слоя смешения, так как эта модель не достаточно верно описывает гидродинамику в промежуточном слое между областью смешения и устойчивой областью.